Induction Bending Effects on Mechanical Properties and Corrosion Resistance of Duplex Stainless Steel UNS S31803 Pipes

Pedro Soucasaux Pires Garcia (psukazo@gmail.com)
Universidade Federal do Rio de Janeiro Centro de Ciencias Matematicas e da Natureza
https://orcid.org/0000-0002-8628-9727
Juan Manuel Pardal
Sérgio Souto Maior Tavares
Larissa Ribeiro de Souza
Antônio Marcelo Meireles
Mauro Carlos Lopes Souza
Maria Cristina Lopez Areiza
Tabatta Regina de Brito Martins

Research Article

Keywords: Duplex stainless steel, Electromagnetic Induction Bending, Corrosion resistance, Mechanical Properties

Posted Date: March 11th, 2022

DOI: https://doi.org/10.21203/rs.3.rs-1423187/v1

Abstract

Duplex stainless steels are well known austenitic-ferritic alloys which combines good mechanical resistance and excellent corrosion resistance. Due to this fact, this steel family is widely employed in offshore piping applications. However, these alloys require great care in thermomechanical processing, such as welding, since they might present serious decrease in corrosion resistance and toughness at the welded joint when compared to the base metal. Undeniably, welding is one of the major processes employed in pipe and industrial equipment assembly, thus requiring higher expertise and caution in order to achieve the desirable good combination of properties of duplex stainless steel alloys. In this context, induction bending process comes as an efficient alternative to reduce the number of weld joints in piping designs. In this work, induction bent tubes were characterized after bending in temperatures inside and outside the standard recommended range, that is, between 950 and 1150°C. Microstructural characterization, mechanical testing and corrosion tests were performed, indicating that the properties of curved materials remained comparable to a solubilized state. Therefore, the electromagnetic induction bending process proves to be not only a viable tool in thermomechanical processing of these materials, but also more productive.

1. Introduction

Duplex stainless steel (DSS) are corrosion resistant alloys with high mechanical properties when compared with conventional austenitic stainless steel grades, because of the higher Cr, Mo and N content and fine biphasic microstructure, composed by similar parts of austenite and ferrite [1] Thus, this alloy family is employed mainly in petrochemical and offshore industries, where a continuous production operation at critical conditions is required.

DSS are employed in pipes and fittings such as tees and elbows, pressure vessel and other process equipment. To fabricate and assemble such equipment, it is commonly required welding or hot forming. These thermomechanical processes, when poorly selected, might lead to deleterious phases precipitation, but even in cases where the variables and performance of thermomechanical process were considered satisfactory, it is still possible to note a slight decrease in toughness and corrosion resistance at the heat affected zone (HAZ) or weld metal (WM), when compared to the base metal (BM) [2].

In this sense, to prevent mechanical properties and corrosion resistance degradation, the UNS S31803 DSS grade should be heat treated between 1020ºC and 1100ºC, according to ASTM A790 [3]. Therefore, there were selected temperatures of 950ºC, 1060ºC and 1150ºC, to heat the tubes in the bending process, which was carried out in three different speeds: 0.2, 0.5 and 0.8 mm/s. These temperatures were chosen to simulate the influence of an occasional fluctuation below and above the range allowed by the referred standard. To compare the hot bending and solution treated conditions, some samples were induction heated at the same solution treatment temperature for three different treatment times, which were based on the average duration necessary to perform the induction bending tests for each speed.

This work shows that induction bending process in DSS might be used as an alternative to reduce the number of welding joints. The bended pipes presented excellent properties and the process might as well improve productivity in spool assembly. Finally, this process can save time and reduce costs in fabrication and erection activities associated with the supply delay of high diameter duplex forged fittings such as pipe forged bends.

2. Experimental Procedures

This study was performed in the as received (AR) DSS UNS S31803 seamless pipe with 3½ in (88,9 mm) diameter and 19,0 mm wall thickness, after solution treatment condition, which chemical composition is presented at Table 1. Some of the samples where then induction bent (solution treated and bent, identified as STB) and others remained at solution treated (ST) condition for comparison purposes. The bent machine used was a high frequency bending machine Dai-ichi High Frequency Co. Ltd model HR-28GB, with incorporated Yukon automation system. In order to achieve the selected temperatures, the frequency, tension and current applied varied between 1.5–1.8 kHz, 400–700 V and 6.8–8.5 kA, respectively. The induction coil, presented in Fig. 1, had 28 mm of width with 41 mm of lift off. The temperature was monitored by an infrared pyrometer and the cooling was carried out by water spray at room temperature with a pressure of 0.1 kgf/cm². Figure 2 shows the DSS tube curved to 90° with a 4D radius after the induction bending process.

Table 1
– Chemical composition for the UNS S31803 duplex pipe

%C	%Mn	%P	%S	%Si	%Ni	%Cr	%Mo	%N
0,018	0,86	0,022	< 0,0005	0,48	5,24	22,3	3,15	0,18

Three selected bending speeds of 0.2, 0.5 and 0.8 mm/s were analyzed at 950°C, 1060°C and 1150°C. These bending speeds correspond to a strain rate of 0.001, 0.003 and 0.005 seg^{-1}, respectively. Other nine tests were performed without bending in these same temperatures varying only the holding time for 3, 6 and 24 minutes. The cooling rate applied in STB samples were higher than 200°C/min and the cooling rate related to ST samples were higher than 300°C/min. Figures 3 through 8 presents the thermal cycles and speeds imposed by each test.

The test samples were then removed from the cross-section area, as shown in Fig. 9, for the solubilized condition in AR and ST conditions. For induction bent specimens (STB), the samples were removed from the extrados of the curved section to perform microstructural characterization. Metallographic characterizations by Beraha, KOH and oxalic acid were performed to reveal phase proportions and deleterious phases in all conditions. The ferrite phase quantifications were performed by image tool software version 3.0, and the analysis considered the average of 24 images taken in each condition: as received (AR), solution treated (ST) and induction bent (STB).

Brinell hardness tests were performed at the pipe surfaces with a King Portable Brinell's according to ASTM E10 [4]. After proper preparation of the surface by sanding, a load of 3000 kgf was applied with a

10 mm diameter ball. Three Brinell hardness measurements were made and averages were calculated. For conditions AR and ST, any region was considered, but for STB, the measurements were taken by the neutral line of the curve.

The Charpy impact test was conducted at -46°C according to ASTM E23-18 [5], using an impact machine model JBW-300. The specimens with dimensions 55 mm x 10 mm x 10 mm with V-notch were removed in the transverse direction, with the opening of the notch in the radial direction and positioned on the external surface of the straight tubes. The external surface of the extrados was employed for bent tubes.

The critical pitting temperature (CPT) measurements were based in ASTM G150 requirements [6], using a solution of 1 mol of NaCl, without previous deaeration. The solution was heated from 10°C at a rate of 6°C / min. Temperature was verified manually at intervals of 15 seconds, using a digital thermometer. The Omnimetra® PG-3901 galvanostat potentiostat was used to apply a potential of 700 mV_{SCE} to the sample. For each sample studied, three tests were performed and the average of the CPT values was calculated. If the CPT values differed more than 5°C from each other for a single given sample, a retest was carried out to ensure a better result.

3. Results And Discussion

3.1 – Microstructural Characterization

Figure 10 shows the micrographs for the DSS along the tube's length. It is possible to verify the sporadic presence of large austenite islands, as well as large ferrite islands. Therefore, it can be said that the phase distribution along the length of the straight tube in the as received condition is not totally homogeneous. No intermetallic phases were found.

In Fig. 11, it shows the solution treated pipe in three different temperatures for three holding times, totaling nine solubilizing combinations. It is possible to note the presence of large random austenite islands at temperatures of 950 and 1060°C. In solubilized samples at 1150 ° C, the presence of the darker phase, ferrite, is more evident, which indicates a bigger concentration of ferrite at higher temperatures A similar microstructures observation was verified by Jiang et al. [7], which submitted the same DSS in solution treatments between 1000ºC and 1200ºC during 24h. No intermetallic phases were detected with Beraha solution.

Figure 12 shows the micrographs for the induction bent pipes at three temperatures and three different speeds, totaling nine combinations of bending. The Micrographs of curved samples indicated in Fig. 12 shows to be very similar to each other, as noted by [8]. It was shown that the austenitic islands found themselves slightly smaller in curved samples with speed of 0.8 mm/s at the three tested temperatures, corroborating the statements of [9] that high heating rates prevent the grain growth and induce the formation of an ultra-fine microstructure after subsequent rapid cooling. Relatively large islands and

random austenite were observed in curved samples, as well as in solubilized samples. The STB samples did not present a higher ferrite content at 1150ºC, oppositely to ST ones.

The results for the chromium nitride analysis are presented in Fig. 13, for both the solution treated and induction bent specimens at 1150°C. It is possible to observe the presence of chromium nitrides (Cr_2N), indicated by the red arrows in the three samples solubilized by induction heating. It is important to note that the higher the solution treatment time at 1150 ° C, the higher the concentration of chromium nitrides. This is explained by the lower concentrations of austenite, which favors the segregation of nitrogen in the ferrite phase and the precipitation of Cr_2N when cooling. Similar results were also found by [10–12]. The bent tubes (STB) showed a lower amount of chromium nitrides precisely for this reason, as can be seen comparing Figs. 11 and 12, where there was a more prominent presence of the ferrite at 1150ºC for the ST samples.

Figure 14 shows the ST sample at 950°C for 24 minutes and attacked with KOH for sigma phase detection. As can be noted at the referred figure, there were no signs of sigma phase. This result was corroborated by [12, 13], where only treatments for periods longer than 10h started to show appreciable sigma phase amounts.

3.2 – Hardness Measurements

The values of hardness measured for the ST and STB specimens are shown in Fig. 15 and Fig. 16, respectively. By comparing both graphs, it is possible to note that the hardness of the induction bent tubes is relatively smaller than that of the ST condition, regardless of temperature, bending speed and solution time. This is because the specified bending rates suggest a very rapid time of exposure to the three temperatures studied, providing a short time for the samples to reach phase equilibrium at each temperature. This resulted in similar hardness values, all lower than AR, for all curved tubes, regardless of temperature. On the other hand, Collie et al. [12, 14] has reported a hardness increase after induction bending, related majorly to deleterious phase precipitation. The values were higher than the ones allowed by standard, but a solution treatment after bending was sufficient to achieve acceptable values. All measurements were lower than the 290 HB, specified by ASTM A790 [3].

3.3 –Phase Quantification, Toughness and CPT measurements

Figure 17 shows the results for toughness, ferrite concentration and CPT of the solution treated samples at 950°C for 3, 6 and 24 minutes. The dotted line, labelled AR in Fig. 17, identifies the as received condition.

Figure 17 indicates that there were no significant variations in the ferrite concentrations and toughness in the 950°C solubilized samples at all three holding times, when compared to the as received condition. The most obvious variation occurred in the sample that was solution treated for 24 minutes, where it is possible to note a slight decrease in the ferrite concentration and, proportionally, a slight increase in toughness. Regarding the CPT, the solution treated samples presented higher corrosion resistance when

compared to the as received condition. Many studies [13, 15] have demonstrated an inversion relation between the solution treatment time and CPT or impact energy for long periods. However, this has not been observed for durations of less than one hour.

In the case of Fig. 18, it shows the outcomes for toughness, ferrite concentration and CPT for the bent samples at 950°C in 0.2, 0.5 and 0.8 mm/s speeds. The dotted line, labeled as AR in Fig. 18, represents the pipe in the as received condition.

It is evident from the results of Fig. 18, except for the toughness in the bent sample at the speed of 0.5 mm/s, that the values are consistent with each other. The discrepancy in the stated measurement can be explained by the results presented in Fig. 10, where it can be clearly seen that the ferrite concentration varies in the as received condition. In the case of specimen bent in 0.5 mm/s speed, the percentage of ferrite could have varied greatly, causing the discrepant measurement when compared to the other samples. Nevertheless, there was no significant variation between the values of toughness from the other bent samples when compared to the sample as received. The same statement is true for the ferrite content. Finally, the curved samples showed slight increase in pitting corrosion resistance as it increased the bending speed. This result can be explained by the lower time spent at the temperature of 950°C, preventing the precipitation of sigma phase.

Figure 19 shows the results for toughness, ferrite concentration and CPT of the solution treated samples at 1060°C for 3, 6 and 24 minutes.

It is shown in Fig. 19 that the sample solution treated at 1060°C for 6 minutes presented a CPT superior to the other measured, when it was expected to fall due to the reduced absorbed energy at impact test. However, the maximum difference among the CPTs of solubilized samples to 1060°C was 10.9°C which, in practical terms, is not significant.

In the case of Fig. 20, it shows the results for toughness, ferrite concentration and CPT for the bent samples at 1060°C in 0.2, 0.5 and 0.8 mm/s speeds.

Through Fig. 20, it can be noted a small variation between the ferrite concentrations and toughness from the bent samples and the sample as received. However, it is possible to note a slight raise in pitting corrosion resistance with increasing bending speed. This is an advantage of induction bending as manufacture process, when compared with welding, as the latter usually reduces CPT, even when mechanical properties values were acceptable [2, 16]. Moreover, the analysis of Figs. 19 and 20 shows that induction bending at 1060ºC tends to enhance pitting corrosion resistance, toughness and decrease ferrite content when comparing to solution treatments at the same temperature.

Figure 21 shows the results for toughness, ferrite concentration and CPT of the solution treated samples at 1150°C for 3, 6 and 24 minutes.

Figure 21 shows that solubilized samples at 1150°C presented higher values than the sample as received, which is justifiable due to the higher temperature. Both the absorbed impact energy and the CPT showed

lower values than the sample as received, due to the presence of chromium nitrides in the ferrite phase at these samples, as presented in Fig. 13. Similar behavior was also verified by [10, 11, 17]. Summing up, when the same treatment time was considered, an increase in temperature resulted in higher ferrite content with a consequent CPT and toughness reduction.

Finally, Fig. 22 shows the results for toughness, ferrite concentration and CPT for the bent samples at 1150°C in 0.2, 0.5 and 0.8 mm/s speeds.

Through Fig. 22 it can be shown that the bent samples at 1150°C showed CPT values higher than the sample as received, despite evidence of precipitated chromium nitride in the ferritic phase. When comparing the induction heating treatments presented at Fig. 21 with the bent specimens presented in Fig. 22 it comes clear that ST led to rise in ferrite content, which resulted in a reduced absorbed energy and CPT, while induction bending enhances these properties. Some works [12, 14] has displayed that induction bending process could be deleterious to mechanical properties and corrosion resistance, being necessary a solution treatment at 1120ºC for at least 15 min to restore them. However, this work shows that solution treatments at higher temperatures during long times can also result in deleterious effects due to ferrite content increase and consequently chromium nitrides precipitation. Furthermore, it was detected that induction bending improves CPT, toughness and austenite content when compared with induction heating treatment.

4. Conclusions

This work concludes that bending process in a duplex stainless steel tube can be employed satisfactorily in piping assembly during pre-fabrication stages. This statement is true because the hardness, CPT, phases balance and toughness evaluated in 950–1150°C do not change significantly when compared to the as received condition, and its values are all in the range specified by normative entities [3, 18]. Based on the results presented, it is recommended a temperature of 1060°C to perform the bending process. The increase in hot bending speed did not lead to higher hardness, and instead resulted in better corrosion resistance and a more balanced microstructure.

Comparing the results of this work with the welding process as employed in [2], it has advantages in terms of toughness and corrosion resistance (CPT), making it a good alternative to be used in DSS tube assembly.

Declarations

Acknowledgments

This study was financed in part by the Coordenação de Aperfeiçoamento de Pessoal de Nível Superior - Brasil (CAPES) - Finance Code 001, by CNPq and FAPERJ.

a. Funding – Not Applicable

b. Conflicts of interest/Competing interests – Not Applicable

c. Availability of data and material – Not Applicable

d. Code availability – Not Applicable

e. Ethics approval – Not Applicable

f. Consent to participate – Not Applicable

g. Consent for publication – Not Applicable

h. All authors contributed to the study conception and design. Material preparation, data collection was performed by Larissa Ribeiro de Souza, Antônio Marcelo Meireles and Maria Cristina Lopez Areiza. The data analysis was performed by Pedro Soucasaux Pires Garcia, Juan Manuel Pardal and Sergio Souto Maior Tavares. The first draft of the manuscript was written by Pedro Soucasaux Pires Garcia and all authors commented on previous versions of the manuscript. All authors read and approved the final manuscript.

References

1. Gunn RN (2003) Duplex stainless steels: microstructure, properties and applications, 1st Editon. Elsevier
2. Pardal JM, de Souza GC, Tavares SSM et al (2011) Caracterização e avaliação da resistência à corrosão na soldagem de tubulação de aço inoxidável duplex UNS S31803 pelo processo a arco submerso. Soldag Inspeção 16:310–321. https://doi.org/10.1590/s0104-92242011000400002
3. ASTM A790/A790M (2020) Standard Specification for Seamless and Welded. Ferritic/Austenitic Stainless Steel Pipe
4. ASTM Standard E10 (2018) Standard Test Method for Brinell. Hardness of Metallic Materials
5. ASTM E23 (2018) Standard Test Methods for Notched Bar. Impact Testing of Metallic Materials
6. ASTM G150 (2018) Standard Test Method for Electrochemical Critical Pitting Temperature Testing of Stainless Steels and Related Alloys. https://doi.org/10.1520/G0150-18
7. Jiang Y, Sun T, Li J, Xu J (2014) Evaluation of Pitting Behavior on Solution Treated Duplex Stainless Steel UNS S31803. J Mater Sci Technol 30:179–183. https://doi.org/10.1016/j.jmst.2013.12.018
8. Cabrera JM, Mateo A, Llanes L et al (2003) Hot deformation of duplex stainless steels. J Mater Process Technol 143–144:321–325. https://doi.org/10.1016/S0924-0136(03)00434-5
9. WANG QF, ZHANG CY, XU WW et al (2007) Refinement of Steel Austenite Grain Under an Extremely High Degree of Superheating. J Iron Steel Res Int 14:161–166. https://doi.org/10.1016/S1006-706X(08)60072-2
10. Tavares SSM, Terra VF, Pardal JM, Cindra Fonseca MP (2005) Influence of the microstructure on the toughness of a duplex stainless steel UNS S31803. J Mater Sci 40:145–154.

https://doi.org/10.1007/s10853-005-5700-7

11. Moura VS, Lima LD, Pardal JM et al (2008) Influence of microstructure on the corrosion resistance of the duplex stainless steel UNS S31803. Mater Charact 59:1127–1132. https://doi.org/10.1016/j.matchar.2007.09.002
12. Collie G, Black I, Byrne G, Francis R (2010) Deleterious phases resulting from the induction bending of thick-walled super-duplex pipework. Int J Mater Res 101:772–779. https://doi.org/10.3139/146.110331
13. Deng B, Wang Z, Jiang Y et al (2009) Evaluation of localized corrosion in duplex stainless steel aged at 850°C with critical pitting temperature measurement. Electrochim Acta 54:2790–2794. https://doi.org/10.1016/j.electacta.2008.11.038
14. Collie GJ, Black I (2009) Metallurgical aspects of induction-bending thick-walled super duplex pipework. Proc Inst Mech Eng Part L J Mater Des Appl 223:19–29. https://doi.org/10.1243/14644207JMDA230
15. Wang YQ, Yang B, Han J et al (2012) Localized corrosion of thermally aged cast duplex stainless steel for primary coolant pipes of nuclear power plant. Procedia Eng 36:88–95. https://doi.org/10.1016/j.proeng.2012.03.015
16. de Souza GC, da Silva AL, Tavares SSM et al (2014) Avaliação das propriedades mecânicas e da resistência à corrosão em soldas de reparo pelo processo GTAW no aço inoxidável superduplex UNS S32760. Soldag e Insp 19:302–313. https://doi.org/10.1590/0104-9224/SI1904.03
17. de Lacerda JC, Cândido LC, Godefroid LB (2015) Corrosion behavior of UNS S31803 steel with changes in the volume fraction of ferrite and the presence of chromium nitride. Mater Sci Eng A 648:428–435. https://doi.org/10.1016/j.msea.2015.09.092
18. NORSOK M-630 (2020) Material data sheets and element data sheets for piping

Figures

Figure 1

Coil used for induction bending.

Figure 2

DSS tube after the bending process, curved to 90° with a 4D radius.

Figure 3

Thermal cycle for the ST sample at 950ºC

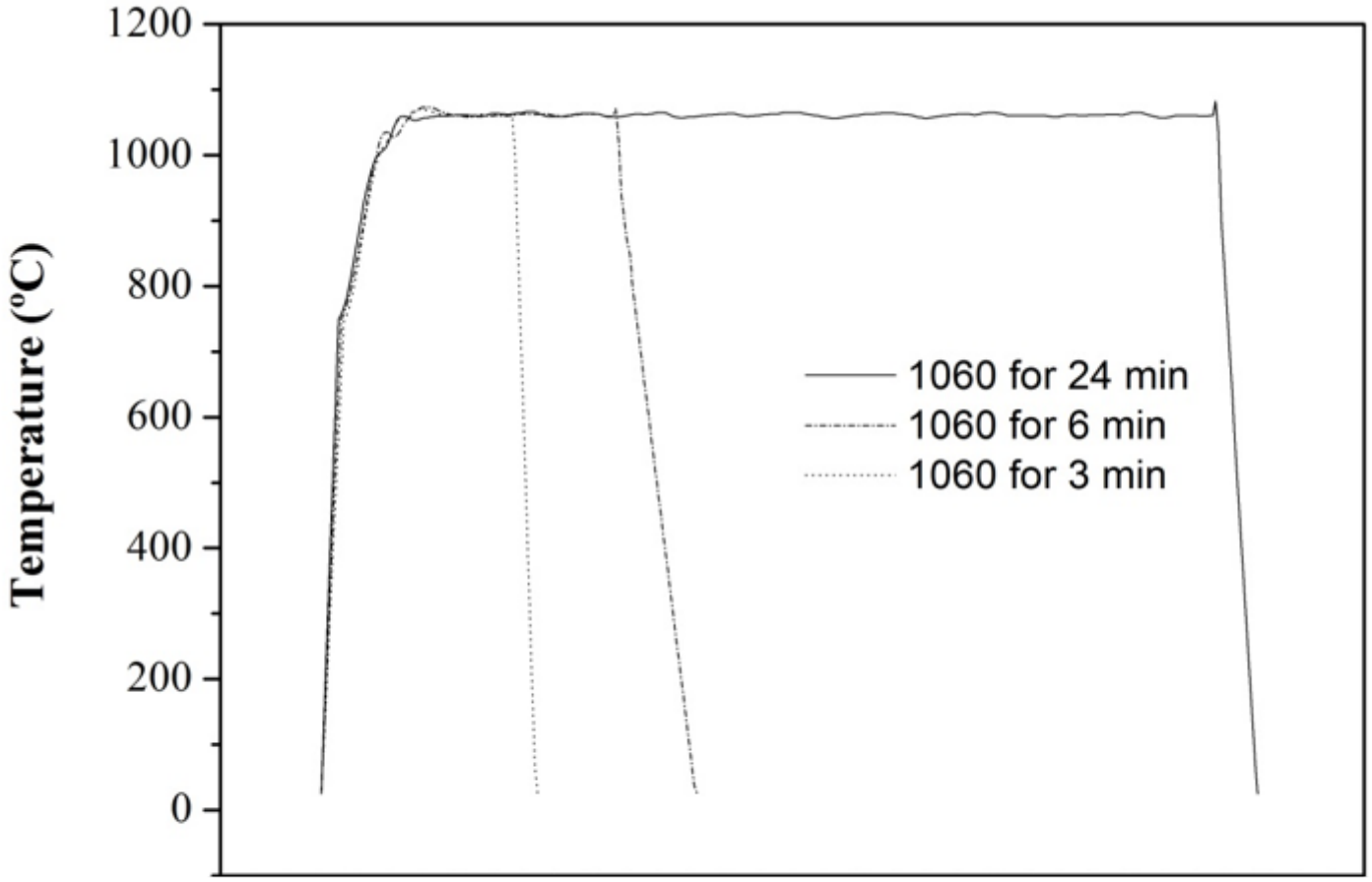

Figure 4

Thermal cycle for the ST sample at 1060ºC

Figure 5

Thermal cycle for the ST sample at 1150ºC

Figure 6

Thermal cycle and bending speed for the STB sample at 950ºC

Figure 7

Thermal cycle and bending speed for the STB sample at 1060ºC

Figure 8

Thermal cycle and bending speed for the STB sample at 1150ºC

Figure 9

Location for the samples removal in the solution treated conditions (a) and induction bent (b) for metallographic characterizations.

Figure 10

Microstructures of AR condition over pipe

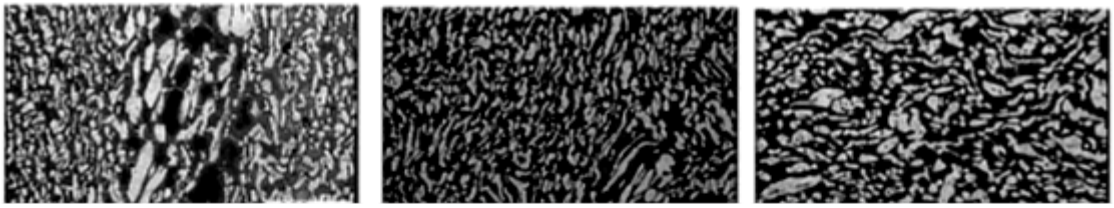

Figure 11

Micrographs of the 99solution treated pipe by induction heating.

Figure 12

Micrographs of the induction bent pipe.

Figure 13

Analysis of chromium nitrides in the solubilized samples and induction bent at 1150°C, revealed by oxalic acid solution.

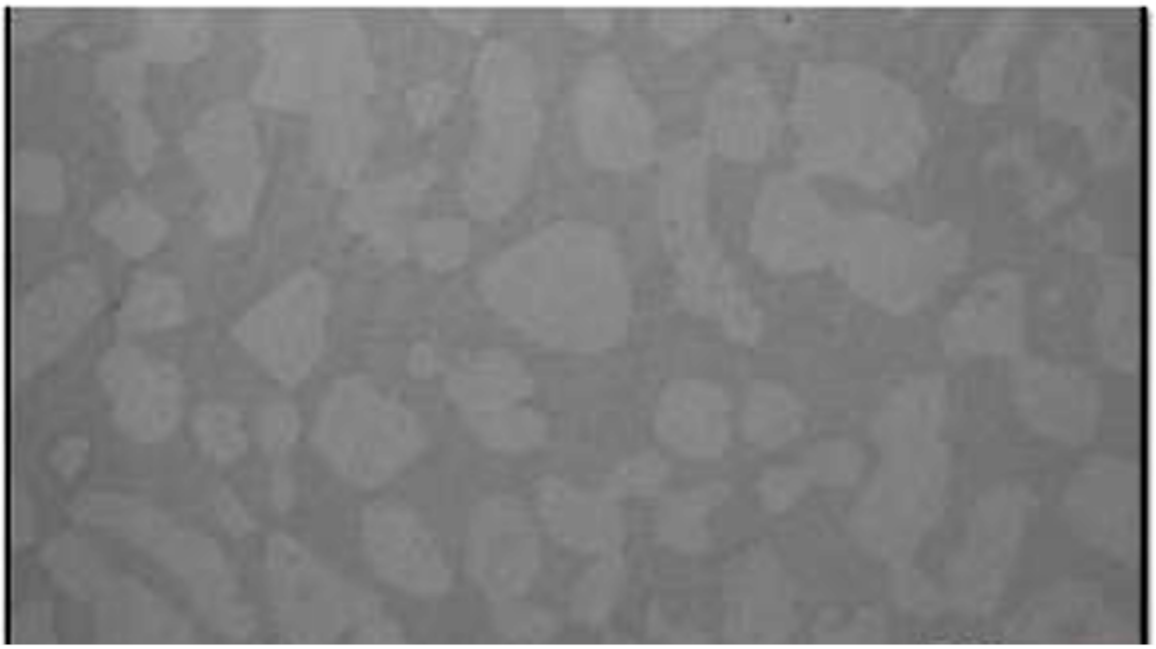

Figure 14

Micrograph of the 950°C for 24 minutes solution treated specimen, electrolytically attacked with KOH.

Figure 15

Hardness values for the ST specimen

Figure 16

Hardness values for the STB specimen

Figure 17

Results for toughness, ferrite concentration and CPT of the solution treated samples at 950°C at different holding times.

Figure 18

Results for toughness, ferrite concentration and CPT for the bent samples at 950°C.

Figure 19

Results for toughness, ferrite concentration and CPT of the solution treated samples at 1060°C at different holding times.

Figure 20

Results for toughness, ferrite concentration and CPT for the bent samples at 950°C.

Figure 21

Results for toughness, ferrite concentration and CPT of the solution treated samples at 1150°C at different holding times.

Figure 22

Results for toughness, ferrite concentration and CPT for the bent samples at 1150°C.